Journal of Catalysis **206,** 91–97 (2002)
doi:10.1006/jcat.2001.3467, available online at http://www.idealibrary.com on IDEAL®

Methane Conversion into Aromatics in a Direct Plasma-Catalytic Process

M. Heintze[1] and M. Magureanu[2]

Institute for Low Temperature Plasma Physics, Friedrich-Ludwig-Jahn-Str. 19, 17489 Greifswald, Germany

Received July 30, 2001; revised October 31, 2001; accepted October 31, 2001

The conversion of methane to aromatic hydrocarbons was investigated in a pulsed microwave plasma at atmospheric pressure in the presence of a heterogeneous catalyst. The influence of the microwave power and methane flow rate or residence time, respectively, on the conversion degree and product concentration was analyzed. The methane conversion reached 60–70%. Higher hydrocarbons were produced, with C_2 being the most abundant. Only after initial carbon formation in the discharge were aromatic products observed. The solid carbon catalyzed the methane aromatization. Benzene was the main aromatic product formed, in concentrations up to 0.6%, with selectivities up to approximately 30%. © 2002 Elsevier Science (USA)

Key Words: **methane conversion; aromatic hydrocarbons; microwave plasma; aromatization; plasma catalysis.**

INTRODUCTION

Natural gas is found in considerable amounts in oil fields, often at remote locations, where the construction of pipelines to transport the gas is not economical. Under these circumstances it is usually flared, vented, or pumped underground. Therefore, finding an efficient process for utilizing such stranded gas receives considerable attention. In this direction, the conversion of methane, the main constituent of natural gas, into more valuable hydrocarbons is a topic of major interest.

Up to now, indirect processes, involving partial oxidation and Fischer–Tropsch synthesis, have been used for this purpose. Recently many attempts have been made to develop a direct process for converting methane into higher aliphatic hydrocarbons as well as aromatics, the effective chemical activation of the methane molecule remaining the most challenging step in such a process.

Plasma excitation was used as an efficient method for the dehydrogenative coupling of methane in the absence of oxygen. C_2 hydrocarbons, mainly acetylene, were obtained in pulsed corona discharges at atmospheric pressure, with high selectivities (70–90%) (1, 2). In a dielectric barrier discharge reactor high selectivities toward ethane were reported (3, 4). In microwave (MW) plasmas the product distribution shifted from ethane for low input energies, to ethylene, and finally to acetylene, the main reaction product at higher power (5, 6). Effective acetylene production was reported in a pulsed microwave plasma (7, 8). As a general trend, low power densities yielded ethane as the most abundant reaction product, while in more energetic conditions, the distribution shifted toward more dehydrogenated products. Only small amounts of C_3 and C_4 hydrocarbons were usually detected and aromatics are not reported.

By introducing catalysts into a microwave discharge an enhancement in product yield was reported (9, 10). Several studies were devoted to the combination of microwave radiation and catalysts, not necessarily involving a gas discharge (11–14). It was suggested that microwave heating of the catalyst could have an important advantage over conventional thermal heating. In all these investigations the major reaction products were C_2 hydrocarbons. Using high microwave power over nickel and activated carbon catalysts, Marun and coworkers detected hydrocarbons up to C_8 in the products and report also the formation of benzene with a selectivity reaching 33% (15), not taking into account the coke formation.

An alternative approach, not involving plasma, which proved to be a quite successful technique for methane conversion into aromatic hydrocarbons is surface catalysis. A recent review was done by Xu and Lin (16). The most attractive results were found for transition metal ion-exchanged HZSM-5. Wang *et al.* reported that benzene was the only hydrocarbon product formed on Mo/HZSM-5 at 973 K, with 7–8% methane conversion (17).

In this paper the formation of aromatics from methane in a pulsed microwave plasma and in the presence of catalysts is investigated. The combination of plasma and surface catalysis could have a synergetic effect, promoting methane activation to form the desired products.

EXPERIMENTAL

The experiment was carried out in a cylindrical quartz reactor of 20-mm diameter, placed in a rectangular waveguide (WR 340; width, 9 cm; height, 4.5 cm), as shown in

---

[1] To whom correspondence should be addressed. Fax: +49 3834 554 301. E-mail: heintze@inp-greifswald.de.

[2] On leave from the Institute of Atomic Physics, NILPRP, Bucharest-Magurele, Romania.

0021-9517/02 $35.00

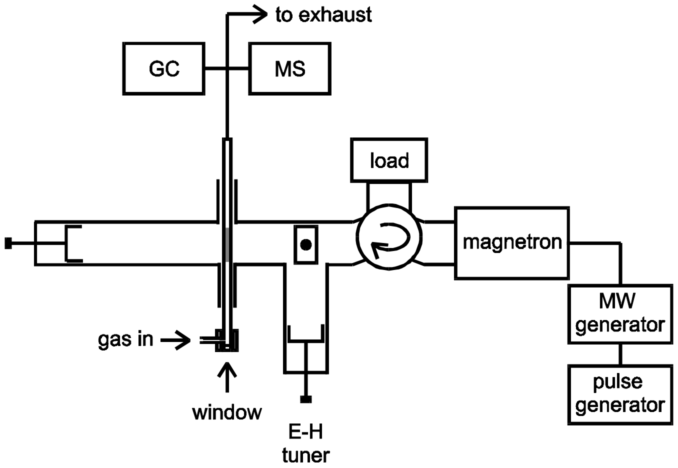

FIG. 1. Experimental setup.

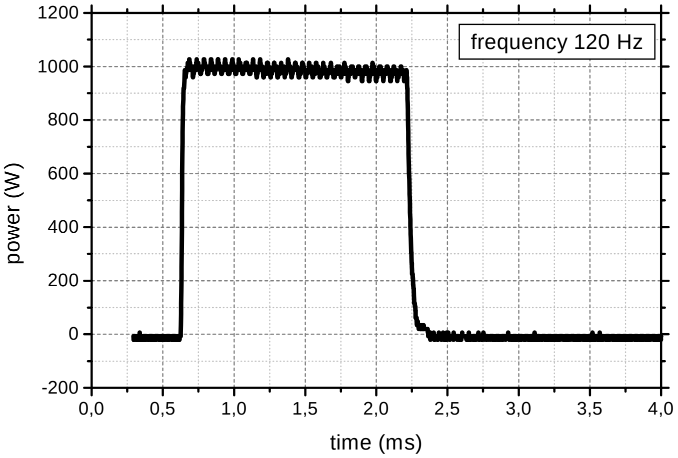

FIG. 2. Typical shape of microwave pulse used in the experiments.

Fig. 1. The tube was positioned through the narrow faces of the waveguide, perpendicular to the electric field. The catalyst contained in the reactor, consisting of short pieces of Ni-wires (approximately 10 mm long; diameter, 0.1–1 mm) embedded in quartz wool, was exposed to pulsed MW radiation. Nickel was used, due to its high efficiency for hydrogen abstraction (18). For comparison, copper, copper oxide, and carbon were also tested. The experiment was carried out at atmospheric pressure under continuous flow of methane, the rate being regulated by flow controllers. Under these conditions discharge sparks appear at the tips of the wires due to local field enhancement.

The MW generator (SAIREM GMP 20 KE/D) supplied up to 2 kW of power at a 2.45-GHz operating frequency. Pulse durations and repetition rates were set by a function generator. The frequency used in the experiments reported here was 120 Hz, and the usual pulse durations were in the range 0.4–2 ms. The forward power was measured internally and the reflected power by a diode probe in the load. Due to its fast response time, this external diode can be used to monitor the input power pulse shape, under conditions of no absorbed power. A typical waveform is presented in Fig. 2. Tuning for minimum reflected power was done with an E–H tuner, which simplifies the operation as compared to a stub tuner and, in combination with silver plating the inner waveguide surfaces, allows transfer of the power to the reactor with negligible loss.

The reaction products were analyzed by gas chromatography and mass spectrometry (MS). The gas chromatograph (column, Poraplot Q; detector, thermal conductivity detector) was calibrated by using test gases with known concentrations (0.1%) of C_1–C_6 hydrocarbons. Ethylene and acetylene were not separated. For benzene and toluene the concentrations were calibrated by saturating the gas phase at given temperatures.

A quadrupole mass spectrometer sampling the gas at the reactor output through a capillary was used to follow the temporal evolution of the conversion degree and product concentrations during the experiments. The following masses were monitored: 2 (hydrogen); 14 (methane); 26 and 27 (contributions from all higher aliphatics); and 78 (benzene). Interference of other hydrocarbons present in the current reaction products with masses 2, 14, and 78 was negligible. Approximate values for the concentrations of acetylene and ethylene were obtained from the ratio of the MS signals for masses 26 and 27. Figure 3 shows the expected contributions of the C_2 and C_3 hydrocarbons to the signals ranging from 24 to 30 for an approximately equimolar mixture. Since in the current experiments the amounts of ethane and C_3 hydrocarbons were much less than that of C_2H_2 and C_2H_4, their contribution to the signals for masses 26 and 27 were neglected and the formula used to estimate the ratio $C_2H_2 : C_2H_4$ was

$$\frac{[C_2H_2]}{[C_2H_4]} = \frac{I_{26} - aI_{27}}{bI_{27}},$$

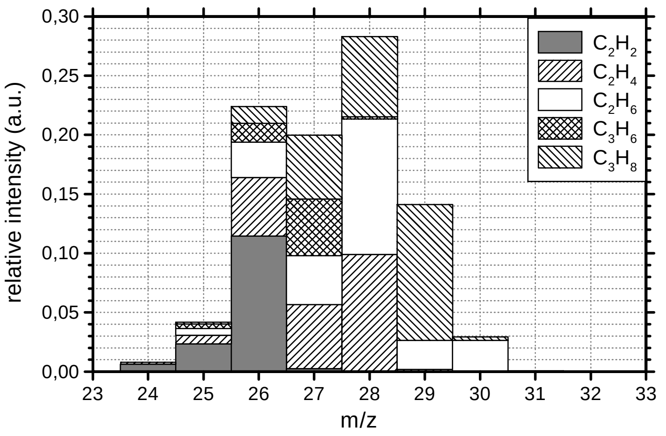

FIG. 3. Contributions of an approximately equimolar mixture of C_2 and C_3 hydrocarbons to MS signals in the range 24–30.

where a and b are constants which depend on the MS and which in our case, from the calibration with test gases, were found to be $a = 0.85$, $b = 1.7$.

The following parameters were investigated.

- Methane conversion (%),

$$X = \left(1 - \frac{CH_4out}{CH_4in}\right) \cdot 100,$$

where CH_4in is moles of methane introduced in the reactor per unit time (flow) and CH_4out is moles of methane at the reactor output. The change in the total flow due to hydrogen formation during the reaction was approximately calculated from the hydrogen balance, taking into account that for every 1 mol of CH_4 converted 1.5–2 mol of H_2 are produced.

- Energy required for methane conversion (eV/molecule),

$$E_{conv}(\mathrm{eV/molec}) = 13.95 \cdot \frac{P_{av}(W)}{CH_4converted\,(sccm)},$$

where P_{av} is the average input power ($P_{av} = P_{peak} \cdot duty\ cycle$) and $CH_4converted$ is moles of methane converted into products ($CH_4converted = CH_4in - CH_4out$).

- Selectivity toward products (%),

$$S(C_xH_y) = x \cdot \frac{C_xH_y}{CH_4converted} \cdot 100,$$

where C_xH_y is moles of compound C_xH_y formed.

RESULTS

Effect of the Amount of Metal Catalyst

In order to investigate the influence of the amount of Ni catalyst introduced in the reactor, the number of wires used was varied between 3 and 30. With a smaller amount of Ni wires the discharge ignition becomes more difficult; however, by proper tuning, a plasma can be obtained with only three wires inside the tube. The methane conversion, the energy required for conversion, and benzene concentrations measured in experiments with three to five wires (#3–5) are compared with those for 25–30 wires (#25–30) in Table 1. The experiments were carried out at a 330-sccm methane flow rate, over a range of average input powers between 96 and 240 W.

It appears that the quantity of metal introduced as catalyst has no influence on the methane conversion and the formation of benzene. This result can be explained by the fact that the plasma is not distributed uniformly inside the tube, but only one or two bright discharge spots appear at the tips of the wires, regardless of the number of wires introduced. Since the methane conversion takes place only in the discharge zone, the lack of effect introduced by different amounts of metal wires is not surprising. In further experiments we used 25–30 Ni wires in the discharge tube.

Near the discharge sparks the temperature will be comparable to values used in surface-catalyzed benzene formation, since in a hydrogen discharge with Ni wires a continuum radiation corresponding to about 1600 K was measured by optical emission spectroscopy.

Catalyst Comparison

In order to compare the catalytic behavior of Ni with other materials, several experiments were made using Cu, CuO, and carbon fiber in the same conditions. Cu and CuO gave similar results as the Ni catalyst. Relatively high methane conversion (up to 50%) could be reached, provided that the average power was high enough and similar selectivities toward the main reaction products were obtained. The selectivities remained in the same range when using carbon fiber as a catalyst, but in this case the methane conversion was slightly smaller compared to the value obtained for Ni and Cu. As far as metal catalysts are concerned, using carbon fibers may be regarded as a blank experiment, since some conductor must be introduced to initiate the discharge.

TABLE 1

Effect of the Amount of Catalyst on Methane Conversion and Benzene Concentration

P_{av} (W)	# 25–30 conv. (%)	# 3–5 conv. (%)	# 25–30 E_{conv} (eV/molec)	# 3–5 E_{conv} (eV/molec)	# 25–30 C_6H_6 (%)	# 3–5 C_6H_6 (%)
96	18.9	12.8	21.5	31.7	0.25	0.18
		17.2		23.6		0.22
144	29.5	38.5	20.6	15.8	0.29	0.34
192	34.5	50.6	23.5	16	0.38	0.44
		43.1		18.8		0.34
240	43.3	40.5	23.4	25.1	0.36	0.38
		33.4		30.4		0.41

Note. For three to five wires, two experiments each are shown at 96, 192, and 240 W.

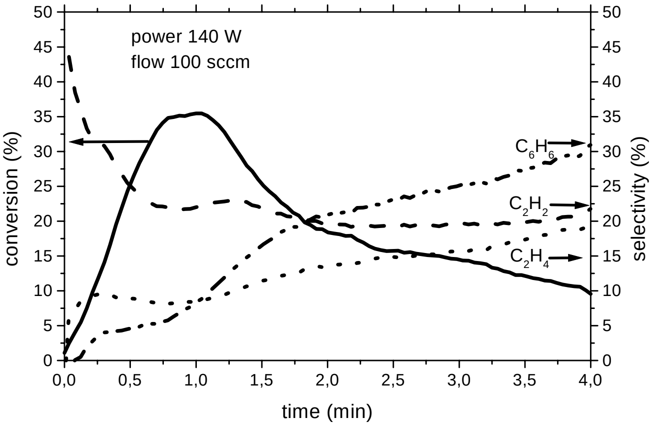

FIG. 4. Methane conversion and product selectivity vs time.

Time Dependence

The evolution of methane conversion and selectivities toward C_2 and benzene during a typical experiment is plotted in Fig. 4. The methane conversion reaches a maximum soon after the discharge is started, then drops to about half of its maximum value and continues to decrease slowly.

Initially, acetylene is formed with a high selectivity, which decreases sharply, then remains almost constant. This decrease coincides with coke formation. Successive experiments performed without changing the catalyst did not show the high initial selectivity toward C_2, indicating the initial decrease in the acetylene selectivity is indeed correlated with the carbon formation. It appears that at maximum conversion a high percentage of the methane is transformed to carbon, and later the carbon formation continues at a smaller rate. Benzene is formed only tens of seconds after starting the plasma. The selectivities toward benzene and ethylene show a continuous increase during the experiment, correlated with the carbon formation.

Effect of Input Power and Flow Rate

The results for a set of experiments performed over a range of average powers between 48 and 320 W and methane flow rates from 40 up to 585 sccm are collected in Table 2. For most experiments the peak power was kept constant (800 W) and the pulse duration was varied between 0.5 and 2 ms. Exceptions are the experiments performed at the highest average powers, where a peak power of 2 kW and pulse durations of 1–1.5 ms were used. Different combinations of peak power–duty cycle showed no effect on the methane conversion and product concentrations in the parameter range tested.

The methane conversion is plotted in Fig. 5 versus the microwave power for three of the methane flow rates used. The other data obtained showed the same tendency, so for clarity they are not represented in the graph. The methane conversion depended approximately linearly on the input power, the highest values ranging between 60 and 70% for

TABLE 2

Effect of the Average Power and Flow Rate on the Conversion and Product Distribution

Flow (sccm)	P_{av} (W)	Conv. max. (%)	E_{conv} (eV/molec)	cC_2 (%)	cC_6H_6 (%)	YC_2 (%)	YC_6H_6 (%)	SC_2 (%)	SC_6H_6 (%)
40	96	32.2	104	1.55	0.14	4.1	1	12.73	3.11
100	48	20.2	33.1	1.69	0.05	4.06	0.37	20.1	1.83
	96	23	58.1	4.4	0.17	10.83	1.25	47.1	5.43
	144	23.7	84.9	1.99	0.33	4.92	2.42	20.76	10.21
	192	45.8	58.5	4.02	0.42	11.72	3.64	25.59	7.95
	240	65.1	51.4	—	0.47	—	4.64	—	7.13
215	48	10.4	30	1.62	0.07	3.58	0.46	34.4	4.42
	96	22	28.3	1.06	0.19	2.59	1.39	11.77	6.31
	192	39.6	31.5	3.94	0.48	11	4.02	27.78	10.15
	240	56.9	27.4	2.85	0.44	8.94	4.14	15.71	7.27
330	48	8.8	23.1	1.02	—	2.22	—	—	26.23
	96	18.9	21.5	2.59	0.25	6.16	1.78	32.59	9.42
	144	29.5	20.6	1.9	0.29	4.92	2.25	16.68	7.63
	192	34.5	23.5	3.63	0.38	9.76	3.07	28.29	8.9
	240	43.3	23.4	2.3	0.36	6.59	3.09	15.22	7.14
470	48	8.3	17.3	1.21	0.01	2.61	0.08	31.44	0.97
	96	9.5	30.1	1.12	0.07	2.45	0.44	25.79	4.63
	144	17.4	24.5	1.9	0.19	4.46	1.35	25.63	7.76
	192	36.2	15.7	3.82	0.36	10.41	2.93	28.76	8.09
	240	35.4	20.1	2.89	0.39	7.83	3.13	22.12	8.84
	320	48.8	19.5	3.18	0.59	9.46	5.25	19.39	10.76
585	96	12.5	18.6	1.36	0.07	3.06	0.5	24.48	4
	320	53.4	14.3	3.32	0.36	10.19	3.3	19.08	6.18

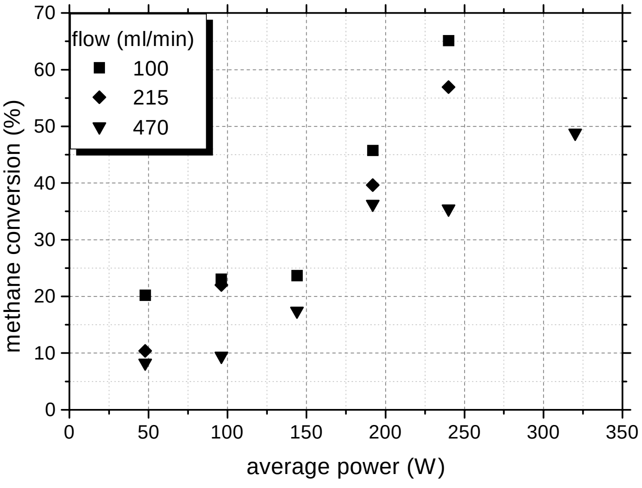

FIG. 5. Maximum methane conversion vs average power.

average powers above 200 W. The influence of the gas flow was much less significant.

As a consequence of the weak variation of conversion with gas flow, the energy required for methane conversion depends essentially on the flow rate, as shown in Fig. 6. Increasing the gas flow over 200 sccm leads to a slow decrease in the conversion energy to values of about 15–20 eV/molecule, where it remains quite independent of the power and of a further increase in the flow rate. This lower limit of the energy required per converted methane is inherent in the plasma excitation and reaction under the present conditions.

The most abundant aromatic formed was benzene. Toluene was detected in concentrations two orders of magnitude smaller than the benzene and xylene only in traces. Figure 7 shows a plot of the benzene concentration vs average power. The benzene concentration in the reaction products depended on the input power in an approximately linear manner and again the methane flow rate did not have a considerable effect. It appears that for the formation of aromatics the input power must be above a threshold value of about 30 W. For lower average power, where methane was converted to some extent, no benzene could be detected.

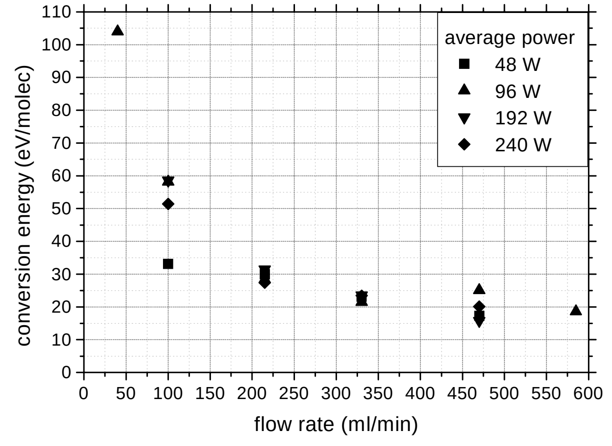

FIG. 6. Energy required for methane conversion vs methane flow rate.

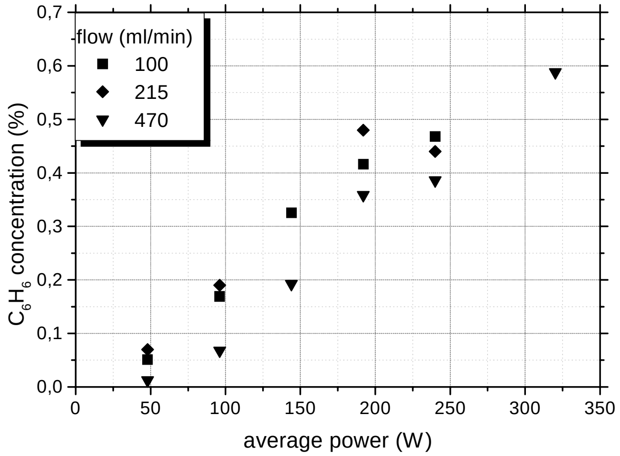

FIG. 7. Benzene concentration vs average power.

The most abundant reaction products detected in these experiments were C_2 hydrocarbons, with only a very small amount of ethane (about 0.1%) and the major part consisting of ethylene and acetylene. The $C_2H_2 + C_2H_4$ concentration increased with the average power, from approximately 1.5% at 48 W to 4–5% at powers over 200 W, only weakly depending on the flow, similar to benzene.

Small amounts of higher aliphatic hydrocarbons were detected, the sum of C_3–C_6 concentrations in the reaction products being less than 0.3–0.4%. The aliphatic products obey the Schulz–Flory law (Fig. 8), which states that the molecular ratios of hydrocarbons with successively higher carbon numbers are constant ($C_{n+1}/C_n = C_{n+2}/C_{n+1}$) (the

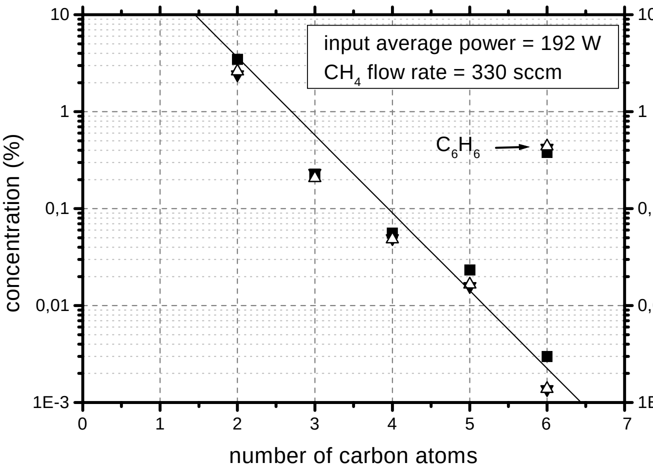

FIG. 8. Product concentrations (sum of saturated and unsaturated C_2–C_6 aliphatics) vs the number of carbon atoms in the product molecule for three experiments in the same conditions.

TABLE 3

Carbon Balance

No.	CH_4 conv. (sccm)	C (sccm)	$C_2H_2 + C_2H_4$ (sccm)	C_6H_6 (sccm)	C_xH_y (sccm)	Σ (sccm)	*r* (%)
1	135	83.6 (62%)	32.5 (24%)	3 (2.2%)	7 (5.2%)	126	93
2	243	157 (64%)	44.5 (18.3%)	8.5 (3.5%)	18.5 (7.6%)	228.5	94
3	79	48 (60%)	15.4 (19.5%)	3.3 (4.2%)	11.4 (14.4%)	78.1	99
4	89	15 (17%)	28 (31%)	2.7 (3%)	20 (22.5%)	66	74

Note. Discharge conditions: 1 and 2, $P_{av} = 192$ W (1.6 kW × 12% duty cycle); 3 and 4, $P_{av} = 80$ W (1.6 kW × 5% duty cycle). Flow = 90 sccm; *r*, $\Sigma/(CH_{4\,conv})$ ratio.

establishment of this distribution requires that methyl radicals be added with equal probabilities to C_2 and higher hydrocarbons, an indication that the chain-growth mechanism is based on the subsequent addition of surface C_1 species). Similar results were obtained under all the experimental conditions studied.

Carbon Balance

Several measurements were made in order to calculate the carbon balance. The total amount of methane converted (CH_4conv) and the amount of methane converted into $C_2H_2 + C_2H_4$ and C_6H_6 were determined by integrating the corresponding MS signals over the duration of the experiment. An approximate estimation for the amount of higher aliphatic hydrocarbons formed (C_xH_y) was obtained from the chromatograms taken during the experiments. The solid carbon formed during the reaction was found by weighing the quartz tube + catalyst before and after the experiment (due to the loss of fibers from the quartz wool during weighing, a simple arrangement using a piece of nickel mesh inside the reactor had to be used in these experiments; the mesh gave similar results as the wires, but with a lower benzene yield). Table 3 shows a reasonably good agreement between the methane converted and the total amount of products formed (Σ—sum of C, C_2H_2 + C_2H_4, C_6H_6, C_xH_y). However, the uncertainty is expected to be in the range of 20%, the most important source of error being the change in total volume and flow rate (due to hydrogen formation during the reaction) which, in these experiments, was not accounted for.

DISCUSSION

In order to understand the benzene formation reported in this paper, both gas phase and surface reactions have to be considered. First the gas-phase activation of methane in a plasma and then its surface catalyzed reactions are reviewed.

Methane activation in a plasma is initiated by collisional processes with energetic electrons. The energy threshold is about 10 eV, comparable to the lower limit of 17 eV per converted methane molecule found in the current results (Fig. 6). The primary reaction path is hydrogen abstraction leading to the formation of CH_3, CH_2, and CH radicals, which react to produce higher hydrocarbons. This process usually leads to a Schulz–Flory distribution, as shown above. Benzene does not follow this distribution and therefore it is highly probable that the actual formation of benzene is a surface process.

Such a surface process is assumed to take place in methane aromatization over MoO_3/ZSM-5. This catalyst was shown to be bifunctional: the active centers for hydrogen abstraction from methane were identified as Mo_2C, formed from MoO_3 by reduction in the initial phase of catalyst operation. Carbon–carbon coupling apparently takes place on the acidic centers of the zeolite. From NMR results it was concluded (19) that sp^2-coordinated carbon formed on the catalyst surface could also be an active surface site for benzene formation. A catalytic activity of some forms of carbon was also established by Murata and Ushijima (20) investigating the methane aromatization over pyrolytic carbon. Another reaction based on hydrogen abstraction over a carbon catalyst is the dehydrogenation of ethylbenzene to styrene (21).

The observed time dependence of the benzene selectivity and its independence on the type of metal introduced indicates that the reaction of the radicals formed in the plasma to benzene is controlled by surface catalysis on the carbon deposited in the vicinity of the discharge sparks.

As an alternative possibility, the mechanism of benzene formation via acetylene trimerization on transition metal catalysts was investigated by a variety of spectroscopic and kinetic methods (22–26). The authors agree upon the acetylene trimerization via a surface C_4 metallocycle, proposing the following pathway for the formation of benzene: acetylene adsorbed on the surface converts into vinylidyne; this can react with gas-phase acetylene to form a C_4H_4 intermediate which was identified on the metal surfaces by NEXAFS (24). The C_4H_4 compound reacts further with acetylene to produce benzene.

However, the formation of benzene in our experiments by direct trimerization of ethylene or acetylene is highly unlikely in view of the temporal evolution of the product selectivities (Fig. 4). If the selectivity toward the final product increases gradually with time, the selectivity toward the intermediate should decrease accordingly. The selectivity toward acetylene is constant after about half a minute and the selectivity toward ethylene actually increases in parallel with the benzene, providing evidence against a mechanism via the C_2 intermediates.

The same conclusion can be drawn from the observed distribution of higher aliphatics. In a study of ethylene metathesis (27), higher hydrocarbons with concentrations following a Schulz–Flory distribution were formed. This was interpreted as the result of the surface dissociation of ethylene and the subsequent chain addition of C_1 species. A Schulz–Flory distribution for higher aliphatics was also found in the present work, strongly supporting the direct chain growth from C_1 species, which are the primary products of methane dissociation in a plasma.

CONCLUSIONS

The results presented here demonstrate the principal feasibility of converting methane into benzene by combining plasma excitation and surface catalysis. The reaction is initiated by plasma activation. The product distribution is controlled by surface catalysis on carbon formed at the beginning of the discharge operation. Methane oligomerization proceeds by chain growth through addition of C_1 radicals formed in the plasma. Acetylene trimerization is therefore an unlikely pathway to benzene here. Benzene formation is very likely to be catalyzed on the coke surface since (i) it is independent of the wire material, (ii) it begins only after some coke is formed, and (iii) such surface catalysis was reported in the literature.

At present the energy input required for the plasma is still far too high for practical applications. This could be overcome if conditions were achieved under which each plasma dissociated methane molecule will lead to the activation of several further molecules through a chain-reaction mechanism (28).

ACKNOWLEDGMENTS

The input and assistance of Shell International E&P B.V. and Prof. J. K. S. Wan, University of Kingston, Ontario, are acknowledged.

REFERENCES

1. Kado, S., Sekine, Y., and Fujimoto, K., *Chem. Commun.* 2485 (1999).
2. Zhu, A., Gong, W., Zhang, X., and Zhang, B., *Sci. China* **43**, 208 (2000).
3. Rutkovsky, J., Drost, H., and Klotz, H.-D., *Proc. ISPC-5* **2**, 765 (1981).
4. Thanychotpaiboon, K., Chavadej, S., Caldwell, T. A., Lobban, L. L., and Mallinson, R. G., *React. Kinet. Catal.* **44**, 2252 (1998).
5. Kopytko, N., and Barronet, F., *Can. J. Chem.* **76**, 1875 (1998).
6. Onoe, K., Fujie, A., Yamaguchi, T., and Hatano, Y., *Fuel* **76**, 281 (1997).
7. Fridman, A., Babaritskyi, A., Jivotov, V., Dyomkin, S., Nester, S., and Rusanov, V., *Proc. ISPC-10* **3**, 1 (1991).
8. Babaritskyi, A., Cheban'kov, F., Jivotov, V., Dyomkin, S., Nester, S., Rusanov, V., and Fridman, A., *VDI Ber*. 1166, 541 (1995).
9. Cho, W., Baek, Y., Park, D., Kim, Y. C., and Anpo, M., *Res. Chem. Intermed.* **24**, 55 (1998).
10. Suib, S. L., and Zerger, R. P., *J. Catal.* **139**, 383 (1993).
11. Wan, J. K. S., U.S. Patent 5472581 (1995).
12. Ioffe, M. S., Pollington, S. D., and Wan, J. K. S., *J. Catal.* **151**, 349 (1995).
13. Fedoseev, V. I., Aristov, Yu. I., Tanashev, Yu. Yu., and Parmon, N. V., *Kinet. Catal.* **37**, 808 (1996).
14. Tanashev, Yu. Yu., Fedoseev, V. I., Aristov, Yu. I., Pushkarev, V. V., Avdeeva, L. B., Zaikovskii, V. I., and Parmon, N. V., *Catal. Today* **42**, 333 (1998).
15. Marun, C., Conde, L. D., and Suib, S. L., *J. Phys. Chem. A* **103**, 4332 (1999).
16. Xu, Y., and Lin, L., *Appl. Catal. A* **188**, 53 (1999).
17. Wang, L., Tao, L., Xie, M., Xu, G., Huang, J., and Xu, Y., *Catal. Lett.* **21**, 35 (1993).
18. Liao, M.-S., and Zhang, Q.-E., *J. Mol. Catal. A* **136**, 185 (1998).
19. Wang, L., Wei, C., Liu, X., Xu, Y., and Guo, X., *Progr. Nat. Sci.* **9**, 109 (1999).
20. Murata, K., and Ushijima, H., *J. Chem. Soc. Chem. Commun.* 1157 (1994).
21. Mestl, G., Maksimova, N. I., Keller, N., Roddatis, V. V., and Schlögl, R., *Angew. Chem.* **113**, 2122 (2001).
22. Logan, M. A., Rucker, T. G., Gentle, T. M., Muetterties, E. L., and Somorjai, G. A., *J. Phys. Chem.* **90**, 2709 (1986).
23. Abdelrehim, I. M., Thornburg, N. A., Sloan, J. T., Caldwell, T. E., and Land, D. P., *J. Am. Chem. Soc.* **117**, 9509 (1995).
24. Ormerod, R. M., Lambert, R. M., Hoffmann, H., Zaera, F., Yao, J. M., Saldin, D. K., Yang, L. P., Bennett, D. W., and Tysoe, W. T., *Surf. Sci.* **295**, 277 (1998).
25. Tysoe, W. T., *Isr. J. Chem.* **38**, 313 (1998).
26. Kaltchev, M., Stacchiola, D., Molero, H., Wu, G., Blumenfeld, A., and Tysoe, W. T., *Catal. Lett.* **60**, 11 (1999).
27. Bartlett, B. F., and Tysoe, W. T., *Catal. Lett.* **44**, 101 (1997).
28. Babaritski, A., Deminskiy, M., Etievant, K., Jivotov, V., Potapkin, B., Rusanov, V., and Ryazantsev, E., *Proc. ISPC-14* **5**, 2289 (1999).